A Novel Control strategy of Modular Multilevel Converter Based on Instantaneous Power Theory

Jianyu Yu
School of Electrical and Electronic Engineering
North China Electric Power University
Beijing, China
yujianyu3210@163.com

Chongru Liu
School of Electrical and Electronic Engineering
North China Electric Power University
Beijing, China
chongru.liu@ncepu.edu.cn

Chao Wang
School of Electrical and Electronic Engineering
North China Electric Power University
Beijing, China
huadianwch@163.com

Bowen Ling
School of Electrical and Electronic Engineering
North China Electric Power University
Beijing, China
lingbowen1995@163.com

***Abstract*—The rapid response characteristics of the power electronic device may aggravate the subsynchronous oscillation, which is closely related to the controller of modular multilevel converter (MMC). When a subsynchronous frequency component is fed into classical d/q decoupling controller, the output signals of the converter will include multiple component of sub- and super-synchronous frequency under such situation. In order to solve the problem that classical controller may increase power oscillation, a new controller based on instantaneous power theory is designed, without phase-lock loop and d/q coordinate transformation. Two different control strategies are simulated separately by MMC-HVDC electromagnetic model on PSCAD/EMTDC and the results show that the use of the proposed control strategy suppresses power fluctuations effectively and improves stability of HVDC system as well.**

Keywords—Instantaneous power theory, modular multilevel converter(MMC), subsynchronous oscillation

I. INTRODUCTION

Flexible DC transmission technology based on voltage source converters, especially modular multilevel converters (MMC), characterized by its active power and reactive power decoupling control, has developed rapidly. With significant advantages in clean energy consumption [1], [2], it has become a solution for wind power integration. However, rapid response characteristics of power electronic devices may induce and aggravate the occurrence of subsynchronous oscillations.

Many research results indicate that subsynchronous oscillations are closely related to converter control systems [3], [4]. Many method are used to analyze the influence of control system parameters on the subsynchronous oscillation, such as time domain simulation method [5]-[7], eigenvalue method [8]-[10], Nyquist stability criterion based on harmonic impedance [11], [12], transfer function method [13] and complex torque coefficient method [14]. However, these theoretical studies focus on the influence of parameter variation on the frequency and damping under the condition of single frequency oscillation, which cannot explain the mechanism of multiple frequency components and their mutual influence.

Many scholars have proposed a variety of methods to suppress the subsynchronous oscillations or reduce the risk of their occurrence. In [15], the harmonic impedance analysis method is used to study the distribution of subsynchronous current in large-scale doubly fed wind farms connected to the MMC-HVDC system, and the additional control strategy based on subsynchronous current suppression is developed. In [16], the circulation control method to improve the stability of the system is presented. The mechanism of oscillation caused by the interaction between wind turbine converter and HVDC system is analysis in [17], and in which, the active damping control method is proposed to effectively reduce the risk of oscillation.

Starting from the transfer function of the MMC converter control system, section II deduces mathematical expression of the output signal in the presence of subsynchronous component, discusses the frequency variety, and explains the reason that why the controller cannot suppress the power oscillation. Considering the high controllability of the output voltage of MMC, section III proposes a control strategy based on instantaneous power theory. The analysis shows that the proposed control strategy can greatly reduce the power fluctuation, and the correctness of the proposed control strategy is verified by digital simulation in Section IV.

II. CONTROL SYSTEM OF MMC

A. *Overview of the Control system*

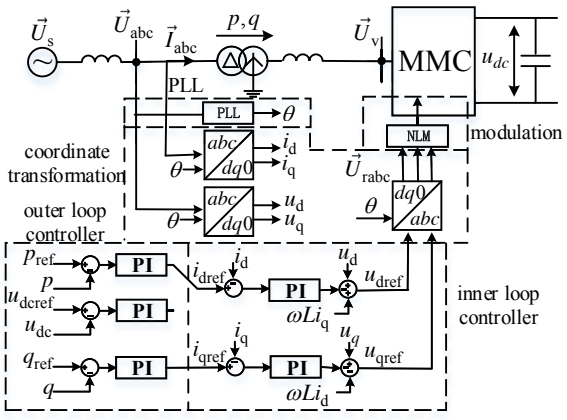

Fig.1 Control block diagram based of MMC

Fig. 1 shows the block diagram of MMC control system mainly including four part which are phase-locked loop (PLL), coordinate transformation, outer and inner loop

978-1-5386-8549-5/18/$31.00 ©2018 IEEE

controller, and modulation. In Fig.1, the phase-locked loop calculates the phase angle of AC bus voltage $\vec{U}_{abc}$ by using coordinate transformation on d-axis and q-axis; inner and outer loop controller realizes decoupling control of active and reactive power and generates three-phase voltage references $\vec{U}_{rabc}$. After modulation, a set of three-phase trigger signals working on the submodule is obtained to ensure that the converter outputs the expected voltage $\vec{U}_v$.

B. Response Characteristics to Subsynchronous Component

1) Coordinate transformation

A Park transformation is performed on three-phase voltage $\vec{U}_{abc}$ with power frequency. The power frequency is ω_0 and rotational frequency of d-axis is ω_θ. The steady-state component U_{d0} on d-axis and U_{q0} on q-axis could be expressed as (1):

$$\begin{bmatrix} U_{d0} \\ U_{q0} \end{bmatrix} = \begin{bmatrix} U_0 \cos(\omega_\theta t - \omega_0 t + \varphi_\theta - \varphi_0) \\ U_0 \cos(\omega_\theta t - \omega_0 t + \varphi_\theta - \varphi_0 + \pi/2) \end{bmatrix} \tag{1}$$

where, U_0 and φ_0 are the amplitude and phase angle of phase voltage with power frequency, respectively. $\theta = \omega_\theta t + \varphi_\theta$ and φ_θ is the phase angle of d-axis.

Assuming that there are three phase voltage disturbance $\vec{U}_{sabc}$ on three-phase phase voltage $\vec{U}_{abc}$ ignoring high order disturbances, the disturbance components of axis d referred as ΔU_d and q referred as ΔU_q could be obtained as (2).

$$\begin{bmatrix} \Delta U_d \\ \Delta U_q \end{bmatrix} = \Delta\theta \begin{bmatrix} U_{q0} \\ -U_{d0} \end{bmatrix} + \begin{bmatrix} U_s \cos(\omega_\theta t - \omega_s t + \varphi_\theta - \varphi_s) \\ U_s \cos(\omega_\theta t - \omega_s t + \varphi_\theta - \varphi_s + \pi/2) \end{bmatrix} \tag{2}$$

where, ω_s is subsynchronous frequency. U_s and φ_s are the amplitude and phase angle of phase voltage disturbance, respectively. The transformation of negative sequence is similar as the one of positive sequence.

2) Phase-locked loop

As shown in Fig. 2, in the phase-locked loop, PI is used to adjust u_q to zero. Hence, the d-axis is oriented to voltage vector, and the angle of the phase A is accurately tracked.

In the presence of voltage disturbance $\vec{U}_{sabc}$, the disturbance of output angle $\Delta\theta$ could be expressed as:

$$\Delta\theta = (K_p/s + K_I/s^2)\Delta U_q \tag{3}$$

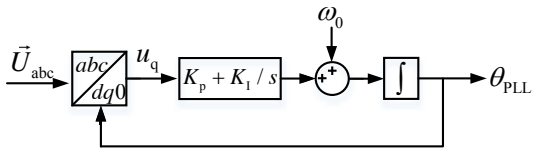

Fig.2 Control block diagram of PLL

where K_p and K_I are the proportion and integral factors respectively in PLL shown in Fig.2.

By substituting (3) into (2), the ripple voltage can be calculated, shown as (4):

$$\begin{bmatrix} \Delta U_d \\ \Delta U_q \end{bmatrix} \approx \begin{bmatrix} U_s \cos(\omega_0 t - \omega_s t + \varphi_0 - \varphi_s) \\ 0 \end{bmatrix} \tag{4}$$

When a three-phase unbalanced component $\vec{U}_{sabc}$ is fed into control system, small ripple will occur at the output of PLL and the d-axis of coordinate transformation as well.

3) Outer and inner loop controller

As shown in Fig. 1, the small signal model of voltage references on d/q axis are:

$$\begin{cases} \Delta U_{dref} = \left[(K_{pd2} + K_{id2}/s)(K_{pd1} + K_{id1}/s)\Delta P \right] + \Delta U_d \\ \Delta U_{qref} = \left[(K_{pq2} + K_{iq2}/s)(K_{pq1} + K_{iq1}/s)\Delta Q \right] + \Delta U_q \end{cases} \tag{5}$$

Where, K_{pd1}, K_{id1}, K_{pq1}, and K_{iq1} are the proportion and integral factors of inner loop controller, respectively; K_{pd2}, K_{id2}, K_{pq2}, and K_{iq2} are the proportion and integral factors of outer loop controller, respectively; ΔP and ΔQ are the first order component caused by subsynchronous voltage $\vec{U}_{sabc}$ working with the current in steady state $\vec{I}_{abc}$.

The voltage references on d/q axis are with same frequency and different amplitude and phase angle, which could be regarded as a superposition of a pair of positive sequence components with frequency of $\omega_0 - \omega_s$ and a pair of negative sequence components with frequency of $\omega_s - \omega_0$. After Park inverse transformation, three-phase voltage references $\vec{U}_{rabc}$ could be expressed as (6):

$$\vec{U}_{rabc} = \vec{U}_{r0} + \Delta\vec{U}_r^+ + \Delta\vec{U}_r^- \tag{6}$$

Where $\vec{U}_{r0}$ is the steady state voltage references with power frequency; $\Delta\vec{U}_r^+$ is the subsynchronous references with frequency of ω_s generated by positive sequence component of d/q axis; $\Delta\vec{U}_r^-$ is the supersynchronous references with frequency of $(2\omega_0 - \omega_s)$ generated by negative sequence component of d/q axis.

4) Summary

The subsynchronous disturbance of grid side is not only fed into the controller through the phase-locked loop and the rotating coordinate transformation, but also brings power oscillation. These two disturbances cause the phenomenon that the converter output superpose synchronization component and supersynchronous component into steady component. Since the amplitude and phase angle of the two components are related to the parameters of the system, the controller cannot effectively suppress the ripple of the power,

and even simultaneously produce multiple frequency components also.

III. Controller Design Based on Instantaneous Power Theory

To ensure the converter output power will not be affected by the subsynchronous disturbance of the grid side, a MMC control strategy based on instantaneous power theory is established and a controller aiming to restrain power ripple component is designed in this section.

The block diagram of MMC control system based on instantaneous power theory shows in Fig. 3. It mainly includes 5 parts: coordinate transformation, power calculation, outer circle controller, inner loop controller and modulation. The power calculation part separates instantaneous active power and instantaneous imaginary power into average components ($\bar{p}$, $\bar{q}$) and oscillating components ($\tilde{p}$, $\tilde{q}$). Then undesired portions of the real and imaginary powers that should be compensated are selected in outer loop controller, wherein voltages that should be compensated are derived. The powers to be compensated are represented by p^* and q^* in the controller shown in Fig. 3, where the voltages to be compensated are represented by u_α^* and u_β^*. The inner loop controller is applied to calculated three-phase voltage references $\vec{U}_{\text{rabc}}$. After modulation, a set of three-phase trigger signals working on the submodule is obtained to ensure that the converter outputs the expected voltage $\vec{U}_{\text{v}}$.

According to the instantaneous power theory, the calculation formula of instantaneous real power and instantaneous imaginary power including the subsynchronous component are as (7):

$$\begin{cases} \bar{p} = 3U_0 I_0 \cos\varphi_0 / 2 \\ \bar{q} = -3U_0 I_0 \sin\varphi_0 / 2 \\ \tilde{p} = 3[U_{\text{s}} I_0 \cos(\omega_0 t - \omega_{\text{s}} t + \varphi_0 - \varphi_{\text{s}}) + \\ \quad U_0 I_{\text{s}} \cos(\omega_0 t - \omega_{\text{s}} t - \varphi_{\text{Is}})] / 2 \\ \tilde{q} = -3[U_{\text{s}} I_0 \sin(\omega_0 t - \omega_{\text{s}} t + \varphi_0 - \varphi_{\text{s}}) + \\ \quad U_0 I_{\text{s}} \sin(\omega_0 t - \omega_{\text{s}} t - \varphi_{\text{Is}})] / 2 \end{cases} \tag{7}$$

In (7), I_{s} and φ_{Is} are the amplitude and phase angle of subsynchronous current respectively.

Under steady condition, $\bar{p} = p_{\text{ref}}$, $\bar{q} = q_{\text{ref}}$, $\tilde{p} = \tilde{q} = 0$.

The compensated voltages calculated by outer loop controller control is:

$$\begin{cases} u_\alpha^* = -\text{K}\dfrac{\sqrt{3}}{\sqrt{2}}\left[U_{\text{s}} \cos(\omega_{\text{s}} t + \varphi_{\text{s}}) + \dfrac{U_0 I_{\text{s}}}{I_0} \cos(\omega_{\text{s}} t + \varphi_0 + \varphi_{\text{Is}}) \right] \\ u_\beta^* = \text{K}\dfrac{\sqrt{3}}{\sqrt{2}}\left[U_{\text{s}} \sin(\omega_{\text{s}} t + \varphi_{\text{s}}) + \dfrac{U_0 I_{\text{s}}}{I_0} \sin(\omega_{\text{s}} t + \varphi_0 + \varphi_{\text{Is}}) \right] \end{cases} \tag{8}$$

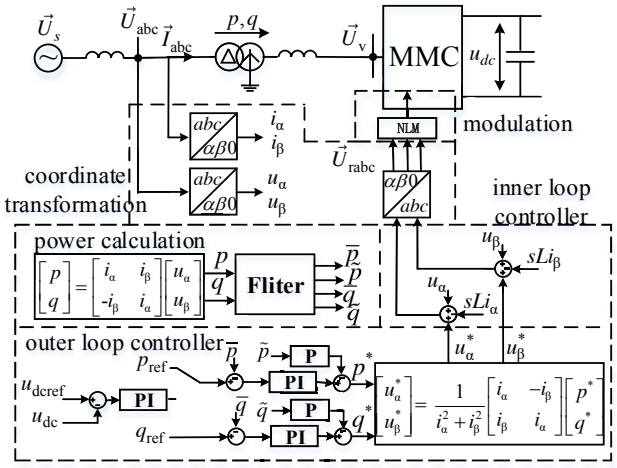

Fig.3 Control block diagram based on instantaneous power theory

Where K is the proportional factor of real power oscillation and imaginary power oscillation. On the right side of the equation, the first term compensates for the power variation caused by the voltage disturbance, and the second term compensates for the power variation caused by the current disturbance.

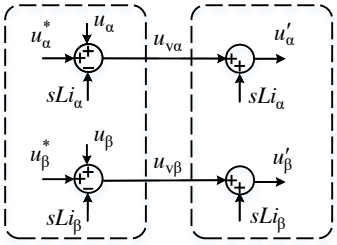

Fig.4 Block diagram of inner loop controller

In Fig. 4, $u_{\text{v}\alpha}$ and $u_{\text{v}\beta}$ are the projections of voltage $\vec{U}_{\text{v}}$ on the α-axis and β-axis. The meaning of u'_α and u'_β are the projections of compensated voltage of the grid side on the α-axis and β-axis. The following equation is obtained:

$$\begin{cases} u'_\alpha = u_\alpha + u_\alpha^* \\ u'_\beta = u_\beta + u_\beta^* \end{cases} \tag{9}$$

Then the compensated power oscillating component is expressed as (10):

$$\begin{cases} \tilde{p}' = 3(1-K)[U_{\text{s}} I_0 \cos(\omega_0 t - \omega_{\text{s}} t + \varphi_0 - \varphi_{\text{s}}) + \\ \quad U_0 I_{\text{s}} \cos(\omega_0 t - \omega_{\text{s}} t - \varphi_{\text{Is}})] / 2 \\ \tilde{q}' = -3(1-K)[U_{\text{s}} I_0 \sin(\omega_0 t - \omega_{\text{s}} t + \varphi_0 - \varphi_{\text{s}}) + \\ \quad U_0 I_{\text{s}} \sin(\omega_0 t - \omega_{\text{s}} t - \varphi_{\text{Is}})] / 2 \end{cases} \tag{10}$$

Comparing the power oscillations in (10) with (7), it can be seen that the controlled power oscillation is (1-K) times of the original one. By selecting the appropriate value of K, the magnitude of the output power variation can be maintained within a small range.

The subsynchronous voltage component of the converter is controlled directly, and the subsynchronous current component is adjusted such that the power oscillation generated by the subsynchronous current and steady state voltage compensates for that generated by the subsynchronous voltage and the steady state current. Therefore, this instantaneous power compensation strategy allows the converter to output stable power in the presence of disturbance.

IV. Simulation and Results

In order to verify the control strategy proposed in Section III, a three-phase-MMC with 226 SMs per arm is established and built on the PSCAD/EMTDC. The main structures of simulation model are shown in Fig. 1 and Fig. 3. The main parameters are listed in Table I.

TABLE I. Main Parameters of MMC-HVDC

Items	Value
Active power rating	1000 (MW)
Rated AC system voltage(L-L, rms)	525 (kV)
Transformer ratio	525 (kV)/262 (kV)
Transformer leakage inductance(secondary side)	44 (mH)
Rated DC voltage	±500 (kV)
Number of SMs per arm	226
SM capacitance	15 (mF)
Arm inductance	75 (mH)

There are two cases simulating respectively with subsynchronous disturbance or without subsynchronous disturbance under classical d/q decoupling control strategy and novel control strategy based on instantaneous power theory.

A. Without subsynchronous disturbance

The simulation model is set as follows: Initially, the active power is set to 1000 MW and the reactive power is set to 300 Mvar. The active power is changed at t = 0.5 s, from 1000 MW to 750 MW. Then, at t = 1.5 s, the active power step from 750 MW to 1000MW. The simulation results of two different control strategies are shown in Fig. 5.

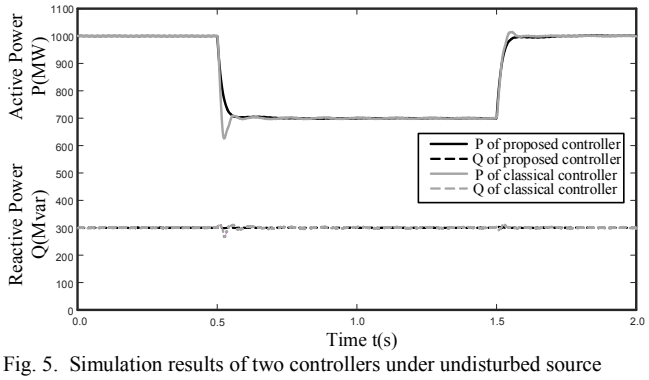

Fig. 5. Simulation results of two controllers under undisturbed source condition

It can be drawn from simulation diagram that there is a relatively long time oscillation and a relatively lager overshoot during the dynamic process when classical control strategy is adopted. However, when adopted the control strategy put forward in this paper, dynamic response process is relatively slow which could decrease the overshoot to a tiny value, and the damping effect to power change is conductive to stability.

B. With subsynchronous disturbance

The simulation result under subsynchronous disturbance shows in Fig. 6. A three-phase positive sequence voltage disturbance is in series with voltage source of grid side, with amplitude of 70 kV and frequency of 30 Hz. Voltage disturbance starts at t = 0.5 s and is removed at t = 1.5 s. Classical controller is switched at t = 1 s whereas the proposed controller put into system.

After switching the controller, the suppression of power fluctuation is obvious, and the amplitude of the subsynchronous power oscillation with frequency of 20 Hz is reduced, which is produced by the interaction between steady current and voltage disturbance. As the disturbance is cleared, the system returns to a steady state, and the power does not include the subsynchronous component. The simulation results show that the proposed control strategy can effectively stabilize the output power of the MMC-HVDC system.

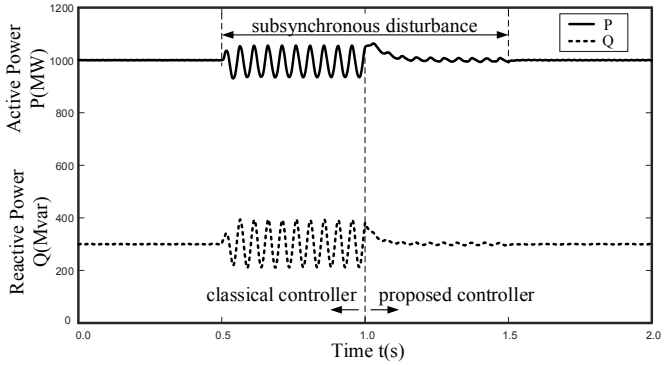

Fig. 6. Simulation results of two controllers under subsynchronous disturbance condition

V. Conclusions

In this paper, small signal mathematical model of each transfer function of MMC controller are presented respectively. It is pointed out in this paper that the multiple frequency phenomenon is generated by the inverter under a subsynchronous frequency component fed into PLL and d/q coordinate transformation. Correspondingly, a controller based on instantaneous power theory is designed and a strategy of suppressing subsynchronous power oscillation is proposed. The following conclusions can be obtained:

1) If there is a subsynchronous component with frequency ω_s feeding into the controller, the converter will generate a subsynchronous component with frequency ω_s and a supersynchronous component with frequency $2\omega_0 - \omega_s$.

2) Based on the d/q decoupling control strategy, the subsynchronous current flowing between the subsynchronous source and subsynchronous component of output of the converter will shift the power fluctuation instead of offset it.

3) The MMC control strategy based on instantaneous power theory has damping characteristics for power variation, which can improve dynamic characteristics of the system and improve system stability. The proposed controller can

effectively suppress subsynchronous power fluctuation and stabilize output power of the converters.

REFERENCES

[1] G. F. Tang, X. Luo, and X. G. Wei, "Multi-terminal HVDC and DC-grid technology," *Proceedings of the CSEE*., vol.33, no.10, pp. 8-17, 2013.

[2] X. X. Zhou, Z. X. Lu, Y. M. Liu, et al, "Development models and key technologies of future grid in China," *Proceedings of the CSEE*, vol. 29, no. 34. pp. 4999-5008, 2014.

[3] J. X. Cai, and M. Molinas, "Frequency domain stability analysis of MMC-based HVDC for wind farm integration," *IEEE Journal of Emerging and Selected Topics in Power Electronics*, vol. 4, no 1, pp. 141-151, 2016.

[4] M. Wu, L. Xie, L. Cheng, et al, "A study on the impact of wind farm spatial distribution on power system sub-synchronous oscillations," *IEEE Transactions on Power Systems*, vol. 31, no. 3, pp. 2154-2162, 2016.

[5] I. Vieto, and J. Sun, "Real-time simulation of subsynchronous resonance in Type-III wind turbines," *2014 IEEE 15th Workshop on Control and Modeling for Power Electronics(COMPEL)*, Santander, Spain, 2014, pp. 1-8.

[6] U. Karaagac, S. O. Faried, J. Mahseredjian, et al, "Coordinated control of wind energy conversion systems for mitigating subsynchronous interaction in DFIG-based wind farms," *IEEE Transactions on Smart Grid*, vol. 5, no. 5, pp. 2440-2449, 2014.

[7] L. Fan, C. Zhu, Z. Miao, et al, "Modal analysis of a DFIG-based wind farm interfaced with a series compensated network," *IEEE Transactions on Energy Conversion*, vol. 26, no. 4, pp. 1010-1020, 2011.

[8] A. E. Leon, "Integration of DFIG-based wind farms into series-compensated transmission systems," *IEEE Transactions on Sustainable Energy*, vol. 7, no. 2, pp. 451-460, 2016.

[9] A, Ostadi, A, Yazdani, and R. K. Varma, "Modeling and stability analysis of a DFIG-based wind-power generator interfaced with a series-compensated line," *IEEE Transactions on Power Delivery*, vol. 24, no. 3, pp.1 504-1514, 2009.

[10] H. A. Mohammadpour, and E. Santi, "SSR damping controller design and optimal placement in rotor-side and grid-side converters of series-compensated DFIG-based wind farm," *IEEE Transactions on Sustainable Energy*, vol. 6, no. 2, pp. 388-399, 2015.

[11] L. Fan, and Z. Miao, "Nyquist-stability-criterion-based SSR explanation for type-3 wind generators," *IEEE Transactions on Energy Conversion*, vol. 27, no. 3, pp. 807-809, 2012.

[12] P. H. Huang, E. Moursi, M Shawky, et al, "Subsynchronous resonance mitigation for series-compensated DFIG-based wind farm by using two-degree-of-freedom control strategy," *IEEE Transactions on Power Systems*, vol. 30, no. 3, pp. 1442-1454, 2015.

[13] H. Xie, B. Li, C. Heyman C, et al, "Subsynchronous resonance characteristics in presence of doubly-fed induction generator and series compensation and mitigation of subsynchronous resonance by proper control of series capacitor," *IET Renewable Power Generatio*n, vol. 8, no. 4, pp. 411-421, 2014.

[14] X. L. Dong, X. R. Xie, Y. D. Han, et al, "Mechanism study of DFIG-related SSR based on separate stator and rotor torque analysis," *Proceedings of the CSEE*, vol. 35, no. 19, pp. 4861-4869, 2015.

[15] J. Lv, P. Dong, G. Shi, et al, "Subsynchronous oscillation and its mitigation of MMC-Based HVDC with large Doubly-Fed Induction Generator-Based wind farm integration," *Proceedings of the CSEE*, vol. 35, no. 19, pp. 4852-4860 2015.

[16] J. Lv, X. Cai. Z. K. Zhang, et al, "Impedance modeling and stability analysis of MMC-based HVDC for offshore wind farms," *Proceedings of the CSEE*, vol. 36, no. 14, pp. 3771-3780, 2016.

[17] M. Amin, M. Molinas," Understanding the origin of oscillatory phenomena observed between wind farms and HVDC systems," IEEE Journal of Emerging and Selected Topics in Power Electronics, vol. 5, no. 1, pp. 378-392, 2017.